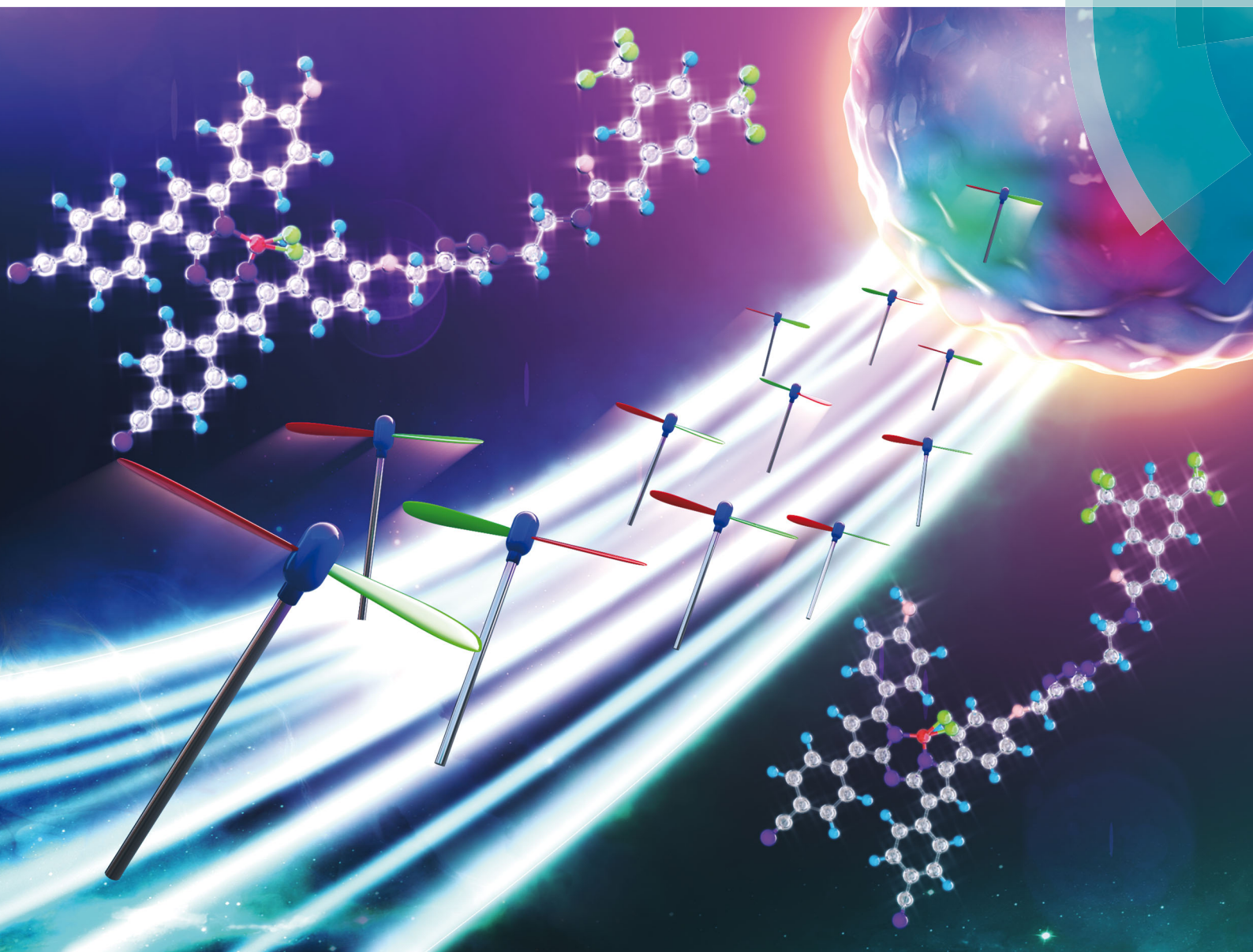


ChemComm

Chemical Communications

rsc.li/chemcomm



ISSN 1359-7345



ROYAL SOCIETY
OF CHEMISTRY

Celebrating
IYPT 2019

COMMUNICATION

Shizhen Chen, Xin Zhou *et al.*

A fluorinated aza-BODIPY derivative for NIR
fluorescence/ ^{19}F MR tri-modality *in vivo* imaging

Cite this: *Chem. Commun.*, 2019, 55, 5851Received 13th February 2019,
Accepted 17th April 2019

DOI: 10.1039/c9cc01253b

rsc.li/chemcomm

A fluorinated aza-BODIPY derivative for NIR fluorescence/PA/¹⁹F MR tri-modality *in vivo* imaging†

Lianhua Liu,^a Yaping Yuan,^a Yuqi Yang,^a Michael T. McMahon,^{bc} Shizhen Chen^{*a} and Xin Zhou  ^{*a}

A fluorinated aza-BODIPY derivative BDPF was developed as a small molecule contrast agent, which displayed highly efficient near infrared fluorescence/photoacoustic/¹⁹F MR tri-modality tumor imaging.

Lung cancer is the most common malignant tumor with the highest incidence and mortality.¹ Therefore, accurate techniques for early diagnosis are highly desirable. Magnetic resonance imaging (MRI) is a widely used non-invasive imaging tool that provides excellent soft-tissue contrast, structural and morphological information.² However, the most commonly used ¹H MRI suffers from significant background signals attributed to abundant endogenous protons.³ In contrast, almost no ¹⁹F MRI signals are observed in living bodies. ¹⁹F atoms mainly exist in the form of solid salts mostly in bones and teeth, and have an extremely shortened transverse relaxation time T_2 .⁴ Moreover, ¹⁹F also offers distinct advantages over other nuclei, including 100% natural abundance, a broad chemical shift range (> 350 ppm) and a high gyromagnetic ratio (40.06 MHz T⁻¹) second only to that of ¹H.⁵ These features provide ¹⁹F MRI with promising potential in MR imaging and spectroscopy studies.⁶

One limitation of ¹⁹F MRI is the relatively poor sensitivity compared with other modalities.⁷ An efficient strategy to overcome this issue is synergistic integration of ¹⁹F MRI with high sensitivity imaging modalities, such as fluorescence imaging and photoacoustic imaging (PAI).⁸ Multimodality imaging could be beneficial to obtain more information about complex pathophysiological processes involved in diseases.⁹

Fluorescence imaging is a popular modality with high sensitivity. Of particular interest are the near infrared (NIR) (650–900 nm) fluorochromes,¹⁰ which have low auto-fluorescence, photon scattering and centimetre-scale imaging depth.¹¹ As one of the NIR dyes, aza-dipyromethene boron difluoride (aza-BODIPY) has gained considerable attention due to its unique photophysical properties.¹² And an assortment of sensors have been constructed for the detection of neutral molecules,¹³ metal cations,¹⁴ anions¹⁵ and pH values.¹⁶ Recently, Tang and co-workers reported an aza-BODIPY-based photosensitizer, exhibiting outstanding PA response.¹⁷ As a new hybrid imaging modality based on optical excitation and ultrasonic detection,¹⁸ PAI is highly suitable for imaging blood vessels and monitoring angiogenesis with high spatial resolution.¹⁹ Therefore, the development of a fluorinated aza-BODIPY derivative that integrates NIR fluorescence, PAI and ¹⁹F MRI into a single molecule is attractive.

A contrast agent bearing tri-modality detectability in a single molecule helps to simultaneously acquire the signal of each modality and ensure identical pharmacodynamics and colocalization.^{20–22} Herein, we developed a small molecule contrast agent based on fluorinated aza-BODIPY for NIR fluorescence/PA/¹⁹F MR tri-modality *in vitro* and *in vivo* imaging (Scheme 1). The contrast agent exhibited excellent photophysical properties with strong absorption and emission wavelengths in the NIR region, and high photostability. Moreover, BDPF also provided good PA absorption at 734 nm. Further, ¹⁹F NMR/MRI measurements of BDPF were performed and revealed a sharp singlet ¹⁹F NMR signal at –63.19 ppm. The longitudinal T_1 and transverse T_2 relaxation times of BDPF were determined to be 836.2 ms and 148.9 ms, respectively. The *in vitro* experiments revealed that BDPF has low cytotoxicity and good biocompatibility.

To achieve tri-modality imaging within a single molecule, aza-BODIPY-based contrast agents BDP and BDPF were designed and synthesized.^{23–26} The detailed synthetic process is illustrated in Scheme S1 (ESI†) and all the compounds were fully characterized (Fig. S11–S28, ESI†).

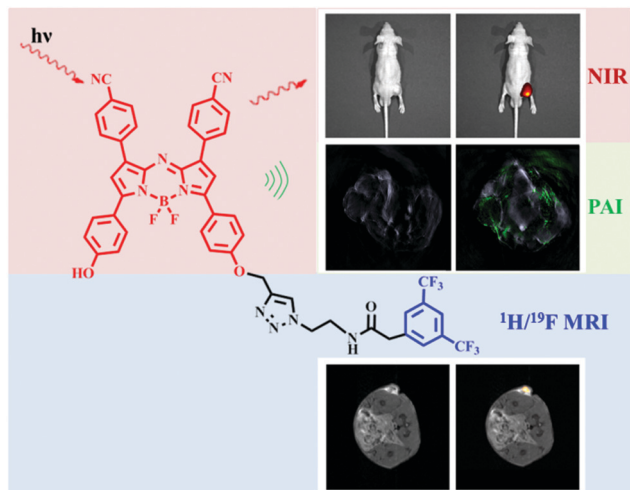
First, the photophysical properties of BDP and BDPF were investigated. As shown in Fig. 1a and b, the maximum absorption

^a State Key Laboratory of Magnetic Resonance and Atomic and Molecular Physics, Wuhan Institute of Physics and Mathematics, Chinese Academy of Sciences, Wuhan National Laboratory for Optoelectronics, Wuhan 430071, China.
E-mail: chenshizhen@wipm.ac.cn, xinzhou@wipm.ac.cn

^b Russell H. Morgan Department of Radiology and Radiological Science, The Johns Hopkins University School of Medicine, Baltimore, Maryland 21287, USA

^c F. M. Kirby Research Center for Functional Brain Imaging, Kennedy Krieger Institute, Baltimore, Maryland 21287, USA

† Electronic supplementary information (ESI) available. See DOI: 10.1039/c9cc01253b



Scheme 1 Tri-modal imaging system for tumor detection.

wavelengths of BDP and BDPF in DMSO were observed at 739 nm and 735 nm, and their maximum emission wavelengths were observed at 779 nm and 780 nm, respectively. In aqueous solution, the maximum absorption and emission wavelengths of BDP and BDPF were both in the NIR region either under acidic (pH = 4.80) or basic (pH = 8.50) conditions (Table 1). However, compared with BDP, BDPF displayed a higher extinction coefficient ($59\,815\text{ M}^{-1}\text{ cm}^{-1}$) and relative fluorescence quantum yield (0.42).

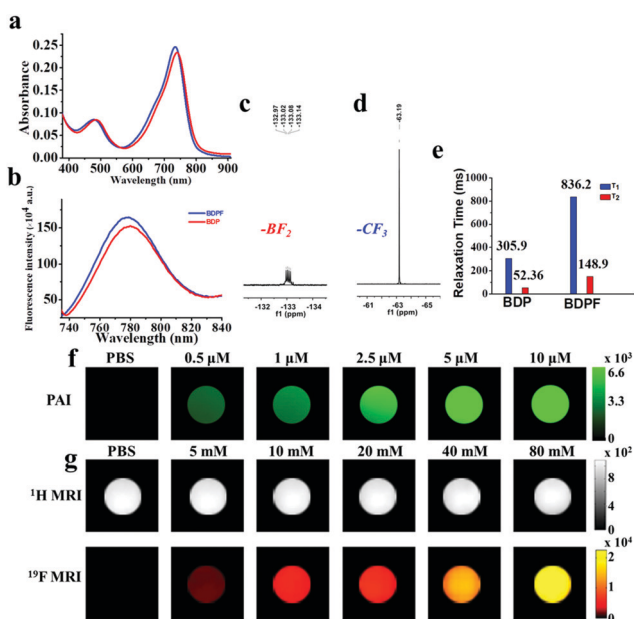


Fig. 1 (a) Absorption spectra of BDP (red) and BDPF (blue) at a concentration of $5\ \mu\text{M}$. (b) Fluorescence emission spectra of BDP (red) and BDPF (blue) at a concentration of $0.5\ \mu\text{M}$. (c) ^{19}F NMR signal of $-\text{BF}_2$ in BDP. (d) ^{19}F NMR signal of $-\text{CF}_3$ in BDPF. (e) Longitudinal T_1 and transverse T_2 relaxation times of $-\text{BF}_2$ and $-\text{CF}_3$ at the same concentration of BDP and BDPF ($0.5\ \text{mM}$). (f) PA images of BDPF at different concentrations ($0.5\ \mu\text{M}$, $1\ \mu\text{M}$, $2.5\ \mu\text{M}$, $5\ \mu\text{M}$, and $10\ \mu\text{M}$). (g) The ^1H and ^{19}F MRI phantom experiments of BDPF solutions at different concentrations (blank, $5\ \text{mM}$, $10\ \text{mM}$, $20\ \text{mM}$, $40\ \text{mM}$, and $80\ \text{mM}$). The images are displayed with two colorimetric scales: ^1H MRI in gray and ^{19}F MRI in pseudocolor.

Table 1 Photophysical properties of BDP and BDPF

Contrast agent	λ_{abs}^a (nm)	$\lambda_{\text{abs-acid}}^b / \lambda_{\text{abs-base}}^b$ (nm)	$\lambda_{\text{F}}^{a,d}$ (nm)	$\lambda_{\text{F}}^{c,d}$ (nm)	ϵ^a ($\text{M}^{-1}\text{ cm}^{-1}$)	Φ_{f}^a
	DMSO	PBS	DMSO	PBS	DMSO	DMSO
BDP	739	733/777	779	775	24 011	0.36 ^e
BDPF	735	734/774	780	776	59 815	0.42 ^e

^a Measured in DMSO. ^b Measured in 20 mM PBS (containing 1% DMSO and 0.1% Cremophor EL (CrEL)). ^c Measured in 20 mM PBS (containing 0.1% DMSO and 0.01% CrEL). ^d Excitation at 720 nm. ^e ZnPtc (Φ_{f} 0.30 in 1% pyridine in toluene) was used as the standard.²⁷

Then we investigated the pH effect on the fluorescence behaviour of BDP and BDPF in PBS buffer. As shown in Fig. S1a and S2a (ESI[†]), the absorption bands of BDP and BDPF showed a blue shift with a decrease in pH from 8.50 to 4.80. Meanwhile, the fluorescence intensity significantly increased 35-fold for BDP and 81-fold for BDPF (Fig. S1b and S2b, ESI[†]). The changes in spectra were attributed to the efficient photo-induced electron transfer as shown in Fig. S3c (ESI[†]).²⁸ Based on the Henderson–Hasselbalch equation,²⁹ the pK_{a} values of BDP and BDPF were calculated to be 6.09 ± 0.02 and 6.72 ± 0.01 (Fig. S3a and S3b, ESI[†]). From these results, we can conclude that these two contrast agents can be used for tumor visualization due to the low pH micro-environment (pH 5.0–6.8).³⁰

Photostability is a critical factor for fluorescent dyes in bioimaging.³¹ Here, the photostability of BDP and BDPF was evaluated by recording the absorption in a time-course manner upon illumination or in the dark. Compared with the commercially available NIR dye indocyanine green (ICG), the absorption intensity of BDP and BDPF decreased slightly after exposure to sunlight or under dark conditions (Fig. S4a, ESI[†]). Even after 5 days, the absorption intensity was more than 95% for BDP and 85% for BDPF. However, the absorption intensity of ICG decreased significantly. Under UV irradiation, the absorption intensity of ICG reduced to 3% within 20 minutes, while for BDP and BDPF 50% intensity was retained for half an hour (Fig. S4b, ESI[†]). These results demonstrated that BDP and BDPF exhibited a much better photostability than ICG.

Furthermore, the PA spectrum of BDPF revealed a broad peak with the maximum intensity at 734 nm (Fig. S4, ESI[†]). Phantoms of different concentrations were investigated by PAI. PBS buffer was used as the control. BDPF solutions at different concentrations used in this study exhibited strong PA signals (Fig. 1f), even at a low concentration of $0.5\ \mu\text{M}$. This could be owing to the high NIR absorption of the contrast agent.

The ^{19}F NMR spectrum of BDP showed quartet peaks centred at 130.97 ppm, $-131.02\ \text{ppm}$, $-131.08\ \text{ppm}$, and $-131.14\ \text{ppm}$ (Fig. 1c), which were ascribed to the ^{11}B – ^{19}F coupling,³² leading to a lower contrast-to-noise ratio (CNR) than that of the singlet peak. Furthermore, the longitudinal T_1 and transverse T_2 relaxation times of BDP were determined to be 305.9 ms and 52.36 ms, respectively. Such above mentioned properties suggested that BDP was not a promising candidate for ^{19}F MRI. Hence, a moiety bearing a bis(tri-fluoromethyl) group was introduced into BDP. The ^{19}F NMR spectrum of BDPF displayed a new signal which gave a sharp singlet peak centred at $-63.19\ \text{ppm}$ (Fig. 1d).

The longitudinal T_1 and transverse T_2 relaxation times of fluorine from the $-\text{CF}_3$ group were measured to be 836.2 ms and 148.9 ms, respectively (Fig. 1e). The above results indicated that BDPF could be a potential candidate for bioimaging.

Then MR imaging was conducted using a 9.4 T micro imaging system.³³ The ^1H MR images showed that the signal intensity of BDPF at different concentrations ranging from 5 to 80 mM was almost consistent with the PBS buffer solution, which was used as the control sample here. However, the ^{19}F MR images showed that the signal intensity displayed a dose-dependent increase, and no signal was observed in the control sample (Fig. 1g). These aforementioned findings revealed that BDPF could be used as a contrast agent for NIR fluorescence/PA/ ^{19}F MR tri-modality imaging.

In vitro experiments: to evaluate the performance of BDPF for *in vitro* imaging, cell experiments were carried out. Time-dependent cellular uptake was determined by incubating A549 cells with BDPF. After 4 hours, obvious red fluorescence was observed in A549 cells, whereas in wi-38 cells, fluorescence was weak (Fig. S8a, ESI[†]). Moreover, the fluorescence intensity of A549 cells was significantly enhanced with increasing BDPF concentration (Fig. S7, ESI[†]). It could be concluded that A549 cells were more efficient in BDPF uptake. Additionally, as shown in Fig. 2a (red color), BDPF was mainly localized to the cytoplasm, which was in accordance with the previously reported results.³⁴

For a contrast agent, its biocompatibility is one of the most important properties for bioimaging. The cytotoxicity of BDPF on A549 cells and wi-38 cells was tested by MTT assay.³⁵ As shown in Fig. S9a (ESI[†]), the cell viability of wi-38 cells and A549 cells was as high as 95% at concentrations ranging from 0.005 to 5 mM. Even at a concentration of 50 mM, the cell viability was up to 90% for wi-38 cells and 88% for A549 cells. Moreover, the cell viability revealed that a solution of 1% DMSO and 0.1% CrEL almost shows no toxicity (Fig. S9b, ESI[†]). These results implied that BDPF has low toxicity and excellent biocompatibility, which facilitated its potential application for further *in vivo* imaging.³⁶

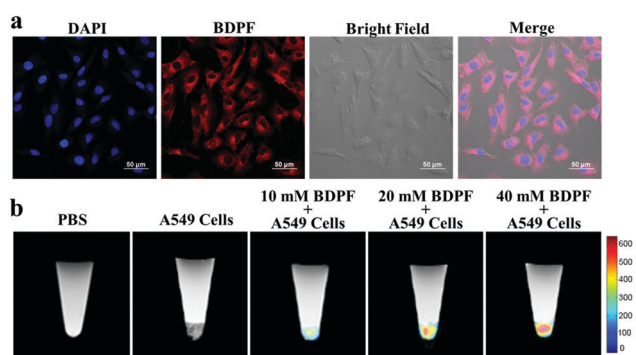


Fig. 2 (a) Confocal laser scanning microscopy images of A549 cells incubated with BDPF (5 μM) for 4 h at 37 $^\circ\text{C}$. Cell images were obtained under excitation at a wavelength of 647 nm. Cell nuclei were stained with DAPI (blue). Scale bar = 50 μm . (b) $^1\text{H}/^{19}\text{F}$ MR images of A549 cells incubated with different concentrations of BDPF (0 mM, 10 mM, 20 mM, 40 mM). The images are shown using two colorimetric scales: ^1H MRI in gray and ^{19}F MRI in pseudocolor.

Next, *in vitro* ^{19}F MR imaging was performed on A549 cells.³⁷ As shown in Fig. 2b, PBS buffer and untreated A549 cells only revealed an ^1H MRI signal. For the other testing samples, the pellet in the tube showed an obvious ^{19}F MRI signal, which was enhanced with increasing BDPF concentration. These results proved that BDPF could be internalized well by A549 cells which were in harmony with the *in vitro* NIR fluorescence imaging results as shown in Fig. 2a.

In vivo NIR fluorescence/PA/ ^{19}F MR tri-modality imaging: furthermore, BDPF was applied for *in vivo* tri-modality imaging. The experiments were performed on A549 tumor-bearing mice. As shown in Fig. 3a, a remarkable enhancement in the NIR fluorescence intensity around the tumor region was obviously observed. For ^{19}F MRI, the signal was acquired around the tumor within 5 min of injection. ^{19}F MRI was overlaid with anatomical ^1H MRI in the same session. In comparison with ^1H MRI, a distinct difference of the tumor can be observed in ^{19}F MRI after administration of BDPF.

For PA imaging, an attempt was made to explore the performance of BDPF. An obvious PA signal in the tumor was acquired after intravenous injection of BDPF (Fig. 3, right). In addition, the 3D images obtained from animal experiments showed the PA signal enhancement in the tumor within 5 min of injection (Fig. S10, ESI[†]). And it can be seen that a significant increase of the PA signals from 5 to 15 min may be due to aza-BODIPY which is a typical photosensitizer. However, after 20 min, the PA signal intensity decreased and gradually accumulated in the liver.

Finally, the major organs of mice from the control and experiment groups were collected for histological analysis under a Nikon Eclipse Ti-SR microscope (Nikon, Japan).³⁸ No noticeable sign of organ damage was observed in H&E stained organ slices (Fig. 3b),

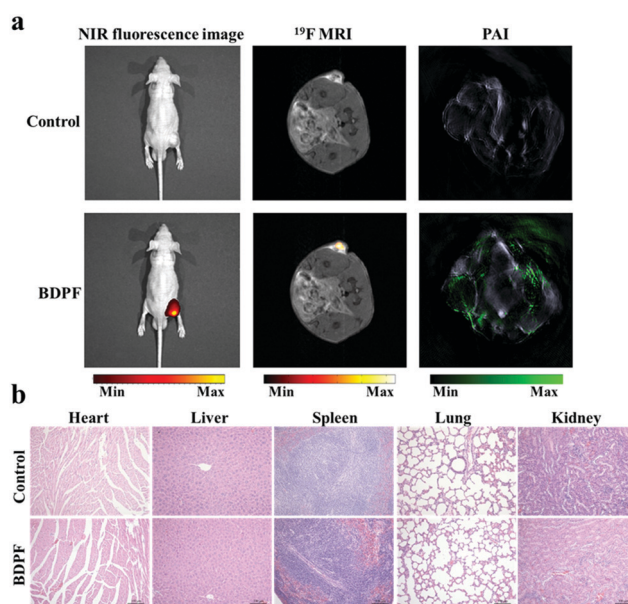


Fig. 3 (a) *In vivo* NIR fluorescence/PA/ ^{19}F MR imaging of a A549 tumor-bearing mouse before and after injection of BDPF. (b) H&E stained images of tissue sections from different organs of the mouse after *in vivo* imaging. Scale bars: 100 μm .

suggesting negligible toxicity and side effects of BDPF for *in vivo* imaging.

In summary, we have developed a fluorinated aza-BODIPY derivative BDPF, which integrates three modalities into a single molecule and can be employed as a tri-modality contrast agent for NIR fluorescence/PA/¹⁹F MR imaging. The contrast agent displayed excellent performance in terms of photophysical, PA and ¹⁹F NMR properties, including a large extinction coefficient, a high relative fluorescence quantum yield, good photostability, a strong PA signal and a sharp singlet ¹⁹F NMR peak. Furthermore, BDPF could be internalized well and localized to the cytoplasm in A549 cells. Cell cytotoxicity assays implied that BDPF has low toxicity which was in favor of its biocompatibility. These advantages of BDPF facilitated its potential application for *in vivo* NIR fluorescence/PA/¹⁹F MR imaging and tumor detection.

This work was supported by the National Natural Science Foundation of China (91859206, 81625011, 21575157, and 21874150), the National Key R&D Program of China (2017YFA0505400 and 2016YFC1304704), the K. C. Wong Education Foundation and Key Research Program of Frontier Sciences, CAS (QYZDY-SSW-SLH018), and the Hubei Provincial Natural Science Foundation of China (2017CFA013).

Conflicts of interest

There are no conflicts to declare.

Notes and references

- 1 G. J. Costa, M. J. G. de Mello, C. G. Ferreira, A. Bergmann and L. C. S. Thuler, *Lung Cancer*, 2018, **125**, 77.
- 2 M. M. Britton, *Chem. Soc. Rev.*, 2010, **39**, 4036.
- 3 Y. Yuan, S. C. Ge, H. B. Sun, X. J. Dong, H. X. Zhao, L. N. An, J. Zhang, J. F. Wang, B. Hu and G. L. Liang, *ACS Nano*, 2015, **9**, 5117.
- 4 Y. Yuan, H. B. Sun, S. C. Ge, M. J. Wang, H. X. Zhao, L. Wang, L. N. An, J. Zhang, H. F. Zhang, B. Hu, J. F. Wang and G. L. Liang, *ACS Nano*, 2015, **9**, 761.
- 5 K. Akazawa, F. Sugihara, M. Minoshima, S. Mizukami and K. Kikuchi, *Chem. Commun.*, 2018, **54**, 11785.
- 6 I. Tirotta, V. Dichiarante, C. Pigliacelli, G. Cavallo, G. Terraneo, F. B. Bombelli, P. Metrangolo and G. Resnati, *Chem. Rev.*, 2015, **115**, 1106.
- 7 S. E. Kirberger, S. D. Maltseva, J. C. Manulik, S. A. Einstein, B. P. Weegman, M. Garwood and W. C. K. Pomerantz, *Angew. Chem., Int. Ed.*, 2017, **56**, 6440.
- 8 X. J. Han, K. Xu, O. Taratula and K. Farsad, *Nanoscale*, 2019, **11**, 799.
- 9 S. Wang, J. Lin, Z. T. Wang, Z. J. Zhou, R. L. Bai, N. Lu, Y. J. Liu, X. Fu, O. Jacobson, W. P. Fan, J. L. Qu, S. P. Chen, T. F. Wang, P. Huang and X. Y. Chen, *Adv. Mater.*, 2017, **29**, 1701013.
- 10 K. Park, Y. Seo, M. K. Kim, K. Kim, Y. K. Kim, H. Choo and Y. Chong, *Org. Biomol. Chem.*, 2015, **13**, 11194.
- 11 X. M. Wu, X. R. Sun, Z. Q. Guo, J. B. Tang, Y. Q. Shen, T. D. James, H. Tian and W. H. Zhu, *J. Am. Chem. Soc.*, 2014, **136**, 3579.
- 12 Y. Ge and D. F. O'Shea, *Chem. Soc. Rev.*, 2016, **45**, 3846.
- 13 N. Adarsh, M. S. Krishnan and D. Ramaiah, *Anal. Chem.*, 2014, **86**, 9335.
- 14 A. Coskun, M. D. Yilmaz and E. U. Akkaya, *Org. Lett.*, 2007, **9**, 607.
- 15 N. Adarsh, M. Shanmugasundaram and D. Ramaiah, *Anal. Chem.*, 2013, **85**, 10008.
- 16 S. O. McDonnell and D. F. O'Shea, *Org. Lett.*, 2006, **8**, 3493.
- 17 Q. Y. Tang, W. L. Si, C. H. Huang, K. K. Ding, W. Huang, P. Chen, Q. Zhang and X. C. Dong, *J. Mater. Chem. B*, 2017, **5**, 1566.
- 18 L. L. Zeng, G. C. Ma, J. Lin and P. Huang, *Small*, 2018, **14**, 1800782.
- 19 Z. D. Guo, M. N. Gao, M. L. Song, Y. S. Li, D. L. Zhang, D. Xu, L. Y. You, L. L. Wang, R. Q. Zhuang, X. H. Su, T. Liu, J. Du and X. Z. Zhang, *Adv. Mater.*, 2016, **28**, 5898.
- 20 A. Louie, *Chem. Rev.*, 2010, **110**, 3146.
- 21 E. Swider, K. Daoudi, A. H. J. Staal, O. Koshkina, N. K. van Riessen, E. van Dinther, I. J. M. de Vries, C. L. de Korte and M. Srinivas, *Nanotheranostics*, 2018, **2**, 258.
- 22 B. Semete, L. Booyesen, Y. Lemmer, L. Kalombo, L. Kantata, J. Verschoor and H. S. Swai, *Nanomedicine*, 2010, **6**, 662.
- 23 X. X. Zhang, Z. Wang, X. Y. Yue, Y. Ma, D. O. Kiesewetter and X. Y. Chen, *Mol. Pharmaceutics*, 2013, **10**, 1910.
- 24 L. P. Jameson and S. V. Dzyuba, *Bioorg. Med. Chem. Lett.*, 2013, **23**, 1732.
- 25 A. Kamkaew and K. Burgess, *Chem. Commun.*, 2015, **51**, 10664.
- 26 J. Murtagh, D. O. Frimannsson and D. F. O'Shea, *Org. Lett.*, 2009, **11**, 5386.
- 27 A. Loudet, R. Bandichhor, K. Burgess, A. Palma, S. O. McDonnell, M. J. Hall and D. F. O'Shea, *Org. Lett.*, 2008, **10**, 4771.
- 28 O. A. Bozdemir, F. Sozmen, O. Buyukcakar, R. Guliyev, Y. Cakmak and E. U. Akkaya, *Org. Lett.*, 2010, **12**, 1400.
- 29 M. H. Lee, N. Park, C. Yi, J. H. Han, J. H. Hong, K. P. Kim, D. H. Kang, J. L. Sessler, C. Kang and J. S. Kim, *J. Am. Chem. Soc.*, 2014, **136**, 14136.
- 30 Y. G. Wang, K. J. Zhou, G. Huang, C. Hensley, X. N. Huang, X. P. Ma, T. Zhao, B. D. Sumer, R. J. DeBerardinis and J. M. Gao, *Nat. Mater.*, 2014, **13**, 204.
- 31 K. Z. Gu, Y. S. Xu, H. Li, Z. Q. Guo, S. J. Zhu, S. Q. Zhu, P. Shi, T. D. James, H. Tian and W. H. Zhu, *J. Am. Chem. Soc.*, 2016, **138**, 5334.
- 32 R. Z. Ma, Q. C. Yao, X. Yand and M. Xia, *J. Fluorine Chem.*, 2012, **137**, 93.
- 33 S. Mizukami, R. Takikawa, F. Sugihara, M. Shirakawa and K. Kikuchi, *Angew. Chem., Int. Ed.*, 2009, **48**, 3641.
- 34 A. Gorman, J. Killoran, C. O'Shea, T. Kenna, W. M. Gallagher and D. F. O'Shea, *J. Am. Chem. Soc.*, 2004, **126**, 10619.
- 35 W. Cao, Y. W. Gu, M. Meineck, T. Y. Li and H. P. Xu, *J. Am. Chem. Soc.*, 2014, **136**, 5132.
- 36 S. Avvakumova, E. Galbiati, L. Pandolfi, S. Mazzucchelli, M. Cassani, A. Gori, R. Longhi and D. Prospero, *Bioconjugate Chem.*, 2014, **25**, 1381.
- 37 B. E. Rolfe, I. Blakey, O. Squires, H. Peng, N. R. B. Boase, C. Alexander, P. G. Parsons, G. M. Boyle, A. K. Whittaker and K. J. Thurecht, *J. Am. Chem. Soc.*, 2014, **136**, 2413.
- 38 J. W. Tian, L. Ding, H. J. Xu, Z. Shen, H. X. Ju, L. Jia, L. Bao and J. S. Yu, *J. Am. Chem. Soc.*, 2013, **135**, 18850.